

# 1 Competition between Solvent–Solvent and Solvent–Solute 2 Interactions in the Microhydration of the Hexafluorophosphate 3 Anion, $\text{PF}_6^- (\text{H}_2\text{O})_{n=1,2}$

4 Yasmeen A. Abdo and Gregory S. Tschumper\*



Cite This: <https://dx.doi.org/10.1021/acs.jpca.0c06466>



Read Online

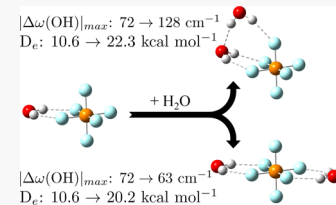
ACCESS |

Metrics & More

Article Recommendations

Supporting Information

**5 ABSTRACT:** This study systematically examines the interactions of the hexafluorophosphate  
6 anion ( $\text{PF}_6^-$ ) with one or two solvent water molecules ( $\text{PF}_6^- (\text{H}_2\text{O})_n$ , where  $n = 1, 2$ ). Full  
7 geometry optimizations and subsequent harmonic vibrational frequency computations are  
8 performed on each stationary point using a variety of common density functional theory methods  
9 (B3LYP, B3LYP-D3, M06-2X, and  $\omega$ B97XD) and MP2 and CCSD(T) *ab initio* methods with a  
10 triple- $\zeta$  correlation consistent basis set augmented with diffuse functions on all non-hydrogen  
11 atoms (cc-pVTZ for H and aug-cc-pVTZ for P, O, and F; denoted as haTZ). Five new stationary  
12 points of  $\text{PF}_6^- (\text{H}_2\text{O})_2$  have been identified, one of which has an electronic energy of  
13 approximately 2 kcal mol<sup>-1</sup>, lower than the only other dihydrate structure reported for this system. The CCSD(T) computations also  
14 reveal that the detailed interactions between  $\text{PF}_6^-$  and  $\text{H}_2\text{O}$  can be quite difficult to model reliably, with some methods struggling to  
15 correctly characterize stationary points for  $n = 1$  or accurately reproduce the vibrational frequency shifts induced by the formation of  
16 the hydrated complex. Although the interactions between the solvent and ionic solute are quite strong (CCSD(T) electronic  
17 dissociation energy  $\approx 10$  kcal mol<sup>-1</sup> for the monohydrate minimum), the solvent–solvent interactions in the lowest-energy  
18  $\text{PF}_6^- (\text{H}_2\text{O})_2$  minimum give rise to appreciable cooperative effects not observed in the other dihydrate minima. In addition, this  
19 newly identified structure exhibits the largest frequency shifts in the OH stretching vibrations for the waters of hydration (with  $\Delta\omega$   
20 exceeding  $-100$  cm<sup>-1</sup> relative to the values for an isolated  $\text{H}_2\text{O}$  molecule).



## 1. INTRODUCTION

21 The hexafluorophosphate anion ( $\text{PF}_6^-$ ) is frequently used as a  
22 component in room temperature ionic liquids (RTILs)<sup>1</sup> and  
23 aprotic electrolytes for lithium-based batteries.<sup>2</sup> In the former  
24 context, the presence of water as an impurity or as a cosolvent  
25 can appreciably alter the physical properties of a given RTIL  
26 (e.g., conductivity, density, solubility, and viscosity).<sup>3–6</sup>  
27 Compared to other common RTILs, those based on  $\text{PF}_6^-$   
28 have been shown to exhibit some of the weakest associations  
29 with water<sup>7</sup> and some of the lowest miscibilities with  
30 water.<sup>8–11</sup>  $\text{PF}_6^-$  is one of the least hygroscopic anions for  
31 RTILs and is generally used to make “hydrophobic” ionic  
32 liquids.<sup>12</sup> As such, the interactions between water with the  
33 ionic components of RTILs containing the hexafluorophos-  
34 phate anion have been the focus of a number of experimental  
35 and computational studies.<sup>6,7,9,13</sup>

36 The  $\text{PF}_6^-$  ion has also played an important role in  
37 fundamental studies of ion solvation in aqueous solutions.<sup>14–21</sup>  
38 Singly deuterated water (HOD) can provide a sensitive  
39 spectroscopic probe of ion hydration. Both Raman and  
40 infrared (IR) measurements have shown that  $\text{PF}_6^-$  shifts the  
41 OD stretching frequency of bulk water (2509 cm<sup>-1</sup>)<sup>22</sup> to  
42 higher energy by more than +150 cm<sup>-1</sup> (ca. 2667 cm<sup>-1</sup>).<sup>14,17</sup>  
43 Recent *ab initio* molecular dynamics (AIMD) simulations by  
44 Smiechowski qualitatively reproduced this result with a  
45 predicted shift of more than +300 cm<sup>-1</sup> for the corresponding

OH stretch.<sup>21</sup> More importantly, the subsequent distance-  
46 dependent analysis of the simulated IR spectrum provided  
47 much needed molecular-level insight into the solute–solvent  
48 interactions that are the source of these unusual perturbations  
49 to the IR spectrum of liquid water.<sup>50</sup>

51 At the smaller end of the size scale for hydration  
phenomena, relatively few microsolvation studies of  $\text{PF}_6^-$   
52 have been carried out with quantum mechanical electronic  
53 structure methods based on wave function theory (WFT) or  
54 density functional theory (DFT). The authors are not aware of  
55 any analogous experimental investigations of small clusters  
56 composed of  $\text{PF}_6^-$  interacting with one or more water  
57 molecules. Two computational studies have examined  $\text{PF}_6^-$   
58 explicitly solvated with one or two water molecules (i.e.,  
59  $\text{PF}_6^- (\text{H}_2\text{O})_{n=1,2}$  clusters) to better understand the water–anion  
60 interaction in RTILs.<sup>12,23</sup> Wang et al. identified a monohydrate  
61 structure (denoted as configuration  $C_{2v}$  edge in Figure 1 of the  
62 present study) and a dihydrate configuration (denoted as  
63 configuration  $D_{2h}$  edge–edge at the top of Figure 2 of the  
64 f2

Received: July 15, 2020

Revised: September 9, 2020

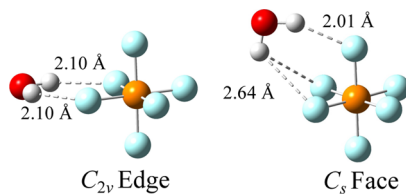


**Figure 1.** CCSD(T)/haTZ-optimized stationary points of  $\text{PF}_6^-(\text{H}_2\text{O})_1$  with select intermolecular  $\text{R}(\text{H}\cdots\text{F})$  distances in Å.

present study).<sup>12</sup> These structures were previously identified as minima on the HF/6-31G\* potential energy surfaces but not with the B3LYP or MP2 methods when using the same 6-31G\* basis set. Rodriguez-Otero et al. published a follow-up study that was able to identify the corresponding minima with both the B3LYP and MP2 methods when using the 6-31+G\*\* basis set.<sup>23</sup> In addition, Rodriguez-Otero et al. identified another monohydrate water structure (denoted herein as configuration  $C_s$  edge and shown in the inset of Figure 3) but only when diffuse functions were not included in the basis set.

In the broader context of ion hydration, the  $C_{2v}$  edge structure (Figure 1) reported for the solvation of  $\text{PF}_6^-$  with a single water molecule is consistent with the double ionic hydrogen bond (DIHB) motif typically observed for molecular anions in the size regime of three or more atoms with the hydrogen bond acceptors separated by at least 2.2 Å.<sup>24–30</sup> The single ionic hydrogen bond (SIHB) pattern is normally reserved for monohydrated atomic and diatomic anions.<sup>30–39</sup>

The progression to dihydrate systems immediately manifests a competition between anion–water and water–water interactions. In the sequence of halide ion dihydrates ( $\text{X}^-(\text{H}_2\text{O})_2$ , where  $\text{X} = \text{F, Cl, Br, and I}$ ), for example, there is essentially no evidence of hydrogen bonding between the two water molecules for  $\text{F}^-$ .<sup>39–44</sup> In contrast, the water–water hydrogen bond is clearly present for the other halide ions, growing in strength from  $\text{Cl}^-$  to  $\text{Br}^-$  and  $\text{I}^-$ ,<sup>39,44–49</sup> but the corresponding spectral signatures can vanish with increasing temperature.<sup>50,51</sup> This competition also extends to other atomic and polyatomic anions.<sup>34,52–56</sup> Interestingly, the  $D_{2h}$  edge–edge structure (Figure 2) identified for the  $\text{PF}_6^-$  dihydrate does not display any sort of solvent–solvent interactions. Instead, the two water molecules independently engage in identical DIHB contacts on opposite edges of the hexafluorophosphate octahedron.<sup>12</sup>

It is worth noting that the closely related sulfur hexafluoride anion ( $\text{SF}_6^-$ ) has been reported to deviate from the aforementioned trends for mono- and dihydrated anions.<sup>57</sup> Although SIHB and DIHB  $\text{SF}_6^-$  monohydrate structures were computed to be nearly isoenergetic (within 0.1 kcal mol<sup>-1</sup>), for this somewhat challenging open-shell system, the IR spectra are more consistent with the former. Similarly, there is no spectroscopic evidence of water–water hydrogen bonding in the dihydrate even though *ab initio* computations suggest that such a structure lies within 0.2 kcal mol<sup>-1</sup> of the lowest-energy  $\text{SF}_6^-(\text{H}_2\text{O})_2$  minimum identified in that study.

The present study builds upon the earlier WFT and DFT results for the  $\text{PF}_6^-(\text{H}_2\text{O})_{n=1,2}$  systems by performing a more extensive exploration of the possible hydration configurations, particularly those exhibiting water–water interactions for  $n = 2$ , utilizing robust *ab initio* methods and correlation consistent basis sets. This investigation also provides a vibrational analysis that complements that of Śmiechowski.<sup>21</sup> Rather than probing spectroscopic perturbations to bulk water, this work examines

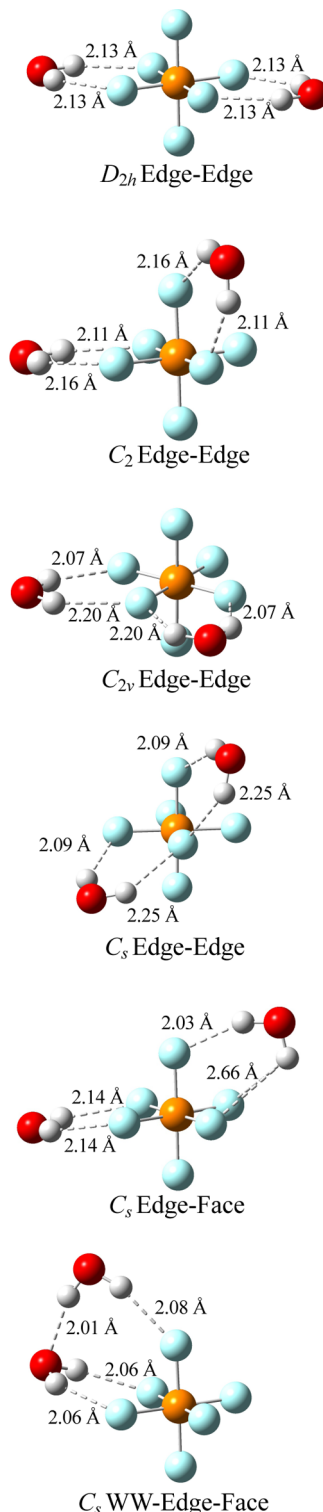


**Figure 2.** CCSD(T)/haTZ-optimized stationary points of  $\text{PF}_6^-(\text{H}_2\text{O})_2$  with select intermolecular  $\text{R}(\text{H}\cdots\text{F})$  and  $\text{R}(\text{H}\cdots\text{O})$  distances in Å.

the shifts in the OH stretching vibrations of an individual  $\text{H}_2\text{O}$  molecule when it interacts with  $\text{PF}_6^-$  (as well as a second  $\text{H}_2\text{O}$  molecule when it interacts to form  $\text{PF}_6^-(\text{H}_2\text{O})_2$ ). In other words, we use an isolated  $\text{H}_2\text{O}$  molecule devoid of intermolecular contacts as the reference for probing the effects of this ionic solute on the (micro)solvent instead of liquid water, which has an extensive network of hydrogen bonds.<sup>124</sup>

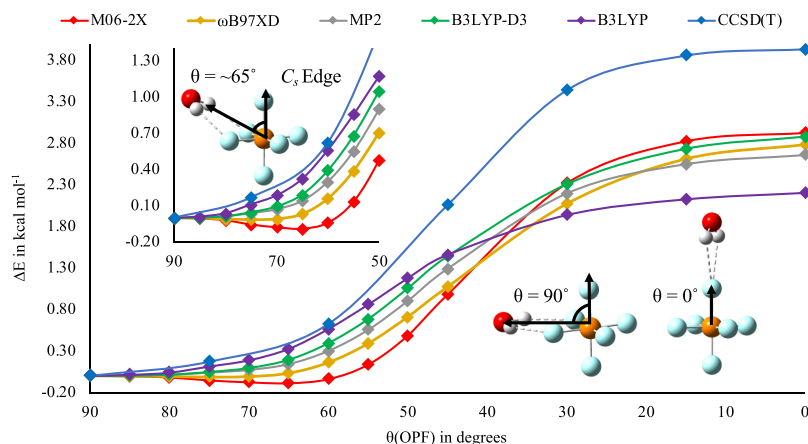


**Figure 3.** Relaxed  $C_s$  scans (with the haTZ basis set) of an  $H_2O$  molecule along a face of  $PF_6^-$  where the scan angle,  $\theta(OPF)$ , is  $90^\circ$  for the  $C_{2v}$  edge configuration (Figure 1) and approximately  $65^\circ$  for the  $C_s$  edge configuration (inset).

**Table 1.** Relative Electronic Energies ( $\Delta E$  in  $kcal\ mol^{-1}$ ) and Number of Imaginary Modes ( $n_i$ ) of the  $PF_6^-(H_2O)_{n=1,2}$  configurations Optimized with Various Methods and the haTZ Basis Set and CCSD(T)/haQZ Relative Energies Computed Using the CCSD(T)/haTZ -Optimized Geometries

structure	$n_i$	CCSD(T)		MP2	B3LYP	B3LYP-D3	$\omega$ B97XD	M06-2X
		haQZ	haTZ					
$C_{2v}$ Edge	$0^a$	+0.00	+0.00	+0.00	+0.00	+0.00	+0.00	+0.00
$C_s$ Face	$1^b$	+0.38	+0.30	+0.34	+0.53	+0.47	+0.15	+0.06
$D_{2h}$ Edge–Edge	$0^c$	+0.00	+0.00	+0.00	+0.00	+0.00	+0.00	+0.00
$C_2$ Edge–Edge	0	+0.08	+0.08	+0.01	+0.01	+0.01	+0.00	-0.18
$C_{2v}$ Edge–Edge	$1^d$	+0.30	+0.29	+0.28	+0.27	+0.27	+0.30	+0.36
$C_s$ Edge–Edge	0	+0.38	+0.33	+0.35	+0.50	+0.37	+0.22	+0.04
$C_s$ Edge–Face	1	+0.37	+0.31	+0.32	+0.47	+0.41	+0.16	-0.04
$C_s$ WW–Edge–Face	0	-2.09	-2.09	-2.11	-1.95	-2.36	-2.48	-2.29

<sup>a</sup> $n_i = 1$  for  $\omega$ B97XD and M06-2X. <sup>b</sup> $n_i = 0$  for  $\omega$ B97XD. <sup>c</sup> $n_i = 3$  for  $\omega$ B97XD and  $n_i = 2$  for M06-2X. <sup>d</sup> $n_i = 0$  for B3LYP and M06-2X.

125 Consequently, the OH vibrational frequency shifts reported  
126 here are in the opposite direction (to lower energy or red-  
127 shifted) from those associated with bulk phase measurements  
128 and simulations (to higher energy or blue-shifted).

## 2. COMPUTATIONAL DETAILS

129 Preliminary relaxed angular scans are performed over several  
130 coordinates of  $PF_6^-(H_2O)_1$  and  $PF_6^-(H_2O)_2$  using various  
131 DFT methods (B3LYP,<sup>58</sup> B3LYP-D3,<sup>58,59</sup> M06-2X,<sup>60</sup> and  
132  $\omega$ B97XD<sup>61</sup>) with Dunning's correlation consistent triple- $\zeta$   
133 basis set augmented with diffuse functions on all nonhydrogen  
134 atoms (cc-pVTZ for H and aug-cc-pVTZ for P, O, and F;  
135 denoted haTZ).<sup>62,63</sup> The resulting low-energy configurations  
136 are then fully optimized with the haTZ basis set and all four  
137 functionals and the MP2<sup>64</sup> and CCSD(T)<sup>65</sup> *ab initio* methods.  
138 All optimizations are computed using analytical gradients. DFT  
139 harmonic vibrational frequencies are computed analytically for  
140 each stationary point, whereas the CCSD(T) Hessians are  
141 obtained from the finite difference of analytical gradients. To  
142 validate the finite difference procedure, MP2 frequencies are  
143 computed both analytically and from the finite difference of  
144 analytical gradients, and the results never differed by more than  
145 0.1  $cm^{-1}$ . Single-point energy computations with the CCSD-  
146 (T) method and the corresponding haQZ basis set are  
147 performed on the CCSD(T)/haTZ geometries using Molpro.  
148 All DFT computations are performed with the Gaussian09<sup>66</sup>  
149 software package with a dense pruned numerical integration  
150 grid composed of 175 radial shells and 974 angular points per

151 shell for H, O, and F and 250 radial shells with 974 angular  
152 points per shell for P corresponding to the superfine keyword  
153 in Gaussian09. MP2 computations are performed using both  
154 Gaussian09 and CFOUR, whereas the CCSD(T) computa-  
155 tions are performed with CFOUR.<sup>67</sup>

156 Analogous optimizations and single-point energy computa-  
157 tions were also performed on the isolated fragments ( $PF_6^-$  and  
158  $H_2O$ ) in order to evaluate the electronic dissociation energies  
159 of the complexes ( $D_e = E[PF_6^-] + nE[H_2O] - E[PF_6^-(H_2O)_n]$ ).<sup>160</sup> This scheme for computing the dissociation  
161 energy and related quantities introduces an inconsistency from  
162 the use of finite basis sets that was identified as early as 1968  
163 by Kestner<sup>68</sup> and later dubbed basis set superposition error  
164 (BSSE).<sup>69</sup> To help assess the impact of this inconsistency on  
165 the  $D_e$  values reported in this work, we apply the popular  
166 counterpoise (CP) procedure developed independently by  
167 Jansen and Ros in 1969<sup>70</sup> and Boys and Bernardi in 1970<sup>71</sup> to  
168 the lowest-energy minima identified for  $n = 1$  and 2. The  
169 extension of the procedure to systems with  $\geq 3$  fragments is not  
170 uniquely defined. For the  $PF_6^-(H_2O)_2$  system, we follow the  
171 protocol described in detail elsewhere<sup>72</sup> for flexible (not rigid)  
172 fragments.

## 3. RESULTS AND DISCUSSION

173 When a water molecule interacts with  $PF_6^-$ , two common  
174 structural motifs are observed for the mono- and dihydrate  
175 stationary points shown in Figures 1 and 2. The “edge” label  
176 for the structures indicates that water has formed two (often  
177

177 symmetric) OH···F contacts with a pair of fluorine atoms along  
178 an edge of the  $\text{PF}_6^-$  octahedron. The “face” label denotes that  
179 water is effectively interacting with the three fluorine atoms at  
180 the vertices of a face on the  $\text{PF}_6^-$  octahedron via one short and  
181 two significantly longer bifurcated OH···F contacts.

182 When two water molecules are present, OH···O contacts  
183 between the water molecules can also occur, which is indicated  
184 by the “WW” designation. This paper will also use the term  
185 hydrogen bonding when referring to these OH···F and OH···O  
186 contacts even though the associated geometrical parameters  
187 might sometimes fall outside the typical ranges associated with  
188 hydrogen bonds involving ions.

### 189 3.1. Monohydrate Structures and Relative Energies.

190 In addition to the  $C_{2v}$  edge minimum reported by Wang, Li,  
191 and Han<sup>12</sup> (left side of Figure 1), a second stationary point has  
192 been identified in the current work for the monohydrated  $\text{PF}_6^-$   
193 system (right side of Figure 1). The  $C_s$  face configuration is a  
194 transition state lying approximately 0.3 kcal mol<sup>-1</sup> above the  
195  $C_{2v}$  structure according to the MP2 and CCSD(T) electronic  
196 energies ( $\Delta E$  values in Table 1).

197 Geometry optimizations with the M06-2X functional and  
198 haTZ basis set readily identify a  $C_s$  edge structure that was  
199 reported in an earlier study when the basis set was not  
200 augmented with diffuse functions<sup>23</sup> (shown in the inset of  
201 Figure 3). However, all subsequent haTZ geometry optimi-  
202 zations with the other methods employed in this study  
203 collapse to the  $C_{2v}$  edge configuration. The relaxed angular  
204 scans shown in Figure 3 along the coordinate connecting the  
205  $C_{2v}$  and  $C_s$  edge structures conclusively demonstrate that the  $C_s$   
206 edge structure does not correspond to a stationary point on the  
207 MP2, CCSD(T), B3LYP, B3LYP-D3, and  $\omega$ B97XD potential  
208 energy surfaces computed with the haTZ basis set.  
209 Consequently, the  $C_s$  edge configuration is not discussed  
210 elsewhere in this report.

211 The scans presented in Figure 3 clearly indicate that some  
212 methods struggle to reliably describe the nature of the  
213 interaction as  $\text{H}_2\text{O}$  adopts different orientations around the  
214 hexafluorophosphate anion. Prior observations<sup>12,23</sup> indicate  
215 that the computational results can also be sensitive to the  
216 quality of the basis set, particularly the presence or absence of  
217 diffuse functions in small double-zeta quality basis sets. In this  
218 work, minor discrepancies are also observed in the number of  
219 imaginary vibrational frequencies ( $n_i$ ) computed for the two  
220 stationary points of this simple monohydrated ion (see  
221 footnotes *a* and *b* in Table 1). The Cartesian coordinates  
222 and harmonic vibrational frequencies for both stationary points  
223 are reported in the Supporting Information for readers  
224 interested in more details.

225 The distance between the F atoms interacting with  $\text{H}_2\text{O}$  in  
226 the  $C_{2v}$  edge structure of  $\text{PF}_6^-(\text{H}_2\text{O})_1$  ( $\approx 2.3$  Å in Figure 1) is  
227 compatible with the distance-based guidelines, suggesting a  
228 propensity for DIHB monohydrate motifs when the atoms  
229 accepting the hydrogen bonds in a polyatomic anion are  
230 separated by at least 2.2 Å.<sup>24</sup> In contrast,  $\text{SF}_6^-$  seems to violate  
231 this relationship because the IR spectrum of its monohydrate is  
232 more consistent with a SIHB structure even though  $\text{SF}_6^-$  is  
233 structurally similar to  $\text{PF}_6^-$  and even has a slightly larger  
234 distance between adjacent F atoms ( $\approx 2.7$  Å).<sup>57</sup> It is also  
235 interesting to note that the F···HO angle about the hydrogen  
236 bond in the  $C_{2v}$  edge structure of  $\text{PF}_6^-(\text{H}_2\text{O})_1$  ( $\approx 142^\circ$  in  
237 Figure 1) is quite similar to a collection of analogous angles for  
238 other DIHB monohydrates ( $146 \pm 2^\circ$  degrees from ref 24)

239 despite being optimized with rather different methods and  
240 basis sets.

241 **3.2. Dihydrate Structures and Relative Energies.** In  
242 addition to the  $D_{2h}$  edge–edge minimum characterized in prior  
243 studies,<sup>12,23</sup> five new stationary points have been identified for  
244 the  $\text{PF}_6^-(\text{H}_2\text{O})_2$  system that have not been reported elsewhere  
245 to the best of our knowledge. All six configurations are shown  
246 in Figure 2. In four of the six structures, both waters bridge an  
247 edge of the  $\text{PF}_6^-$  octahedron. This group includes the  $D_{2h}$   
248 edge–edge minimum, and the other three edge–edge  
249 permutations of the two water molecules along the different  
250 edges of  $\text{PF}_6^-$ . Another dihydrate structure ( $C_s$  edge–face in  
251 Figure 2) was generated from the  $D_{2h}$  edge–edge configuration  
252 by moving one of the water molecules from the edge to an  
253 adjacent face. Other permutations of this hydrogen bonding  
254 motif may exist, but our preliminary optimizations of other  
255 edge–face structures collapsed to one of the aforementioned  
256 edge–edge configurations or to the  $C_s$  WW–edge–face  
257 structure. This new  $C_s$  WW–edge–face configuration exhibits  
258 a completely different hydrogen bonding topology with one  
259 OH···O hydrogen bond between the water molecules along  
260 with three relatively short OH···F hydrogen bonds between the  
261 water molecules and the hexafluorophosphate anion.

262 The  $D_{2h}$  edge–edge structure is adopted as the reference for  
263 the dihydrate relative energies in Table 1 because it has been  
264 previously identified as a minimum for  $\text{PF}_6^-(\text{H}_2\text{O})_2$ .<sup>12,23</sup> The  
265 MP2 and CCSD(T) relative electronic energies in Table 1  
266 indicate that the one edge–face and five edge–edge stationary  
267 points are separated by less than 0.4 kcal mol<sup>-1</sup>. The  $D_{2h}$   
268 edge–edge structure consistently has the lowest electronic  
269 energy, but the nearly isoenergetic  $C_2$  edge–edge lies within  
270 0.1 kcal mol<sup>-1</sup>. However, the electronic energy of the newly  
271 identified  $C_s$  WW–edge–face dihydrate structure is signifi-  
272 cantly lower than that of the  $D_{2h}$  edge–edge by 2.1 kcal mol<sup>-1</sup>  
273 according to the results of the MP2 and CCSD(T) data  
274 reported in the last row of Table 1. These results suggests that  
275 the OH···O (solvent–solvent) interactions between water  
276 molecules may be just as important as the OH···F (solvent–  
277 solute) interactions between water and  $\text{PF}_6^-$  when character-  
278 izing the hydration of this ion.

279 MP2 and CCSD(T) harmonic vibrational frequencies  
280 indicate that all of the edge–edge stationary points are minima  
281 except the  $C_s$  edge–edge structure for which  $n_i = 1$ . The  $C_s$   
282 edge–face configuration is also a transition state, whereas the  
283  $C_s$  WW–edge–face structure appears to be a strong candidate  
284 for the global minimum of the  $\text{PF}_6^-(\text{H}_2\text{O})_2$  system. As with  
285 the monohydrated ion structures, there are some discrepancies  
286 in the number of imaginary vibrational frequencies computed  
287 for the high-symmetry  $D_{2h}$  and  $C_{2v}$  edge–edge dihydrate  
288 stationary points. (See footnotes *c* and *d* in Table 1.) The  
289 Cartesian coordinates and harmonic vibrational frequencies for  
290 all six dihydrate structures are provided in the Supporting  
291 Information.

292 As with the hydration of other molecular anions, water–  
293 water interactions become significant as soon as a second water  
294 molecule is introduced.<sup>34,52,53,55,56</sup> For  $\text{PF}_6^-(\text{H}_2\text{O})_2$ , the  
295 configuration exhibiting water–water hydrogen bonding ( $C_s$   
296 WW–edge–face) lies  $\approx 2$  kcal mol<sup>-1</sup> below that involving only  
297 water–ion interactions. Despite the structural similarities  
298 between  $\text{PF}_6^-$  and  $\text{SF}_6^-$ , the energetics of the dihydrate  
299 systems are quite different. With  $\text{SF}_6^-(\text{H}_2\text{O})_2$ , the IR spectrum  
300 is not consistent with water–water hydrogen bonding, and a  
301

**Table 2.** Dissociation Energies ( $D_e$  in kcal mol<sup>-1</sup>) of the  $\text{PF}_6^-$  Monohydrate and Dihydrate Minima Computed with Various Methods and the haTZ Basis Set and the CCSD(T)/haQZ  $D_e$  Computed Using the CCSD(T)/haTZ-Optimized Geometries

structure	CCSD(T)		MP2	B3LYP	B3LYP-D3	$\omega$ B97XD	M06-2X
	haQZ	haTZ					
$C_{2v}$ Edge	10.55	10.67	10.44	9.16	10.68	10.22	11.00
$D_{2h}$ Edge–Edge	20.17	20.43	19.96	17.43	20.41	19.53	21.00
$C_2$ Edge–Edge	20.09	20.35	19.95	17.41	20.40	19.53	21.18
$C_s$ Edge–Edge	19.80	20.10	19.61	16.92	20.04	19.31	20.96
$C_s$ WW–Edge–Face	22.26	22.52	22.07	19.38	22.78	22.02	23.29

**Table 3.** Shifts in the Harmonic OH Stretching Frequencies ( $\Delta\omega$  in cm<sup>-1</sup>) Induced by Hydrogen Bonding in the  $\text{PF}_6^-$  Monohydrate and Dihydrate Minima Relative to the Symmetric ( $a_1$ ) and Antisymmetric ( $b_2$ ) OH Stretches for an Isolated Water Molecule ( $\omega$  in cm<sup>-1</sup>) Computed with the haTZ Basis Set

irreps <sup>a</sup>	CCSD(T)	MP2	B3LYP	B3LYP-D3	$\omega$ B97XD	M06-2X	H <sub>2</sub> O Frequencies ( $\omega$ )	
							$a_1$	$b_2$
	3814	3825	3801	3801	3882	3872		
	3924	3952	3904	3904	3989	3976		
		$C_{2v}$ Edge Frequency Shifts ( $\Delta\omega$ )						
$a_1$	$a_1$	-17	-27	-27	-32	-28		
$b_2$	$b_2$	-72	-86	-83	-90	-87		
		$D_{2h}$ Edge–Edge Frequency Shifts ( $\Delta\omega$ )						
$b_{3u}$	$a_1$	-13	-22	-22	-26	-24		
$a_g$	$a_1$	-12	-22	-21	-26	-23		
$b_{1g}$	$b_2$	-63	-76	-73	-80	-77		
$b_{2u}$	$b_2$	-62	-75	-72	-79	-76		
		$C_2$ Edge–Edge Frequency Shifts ( $\Delta\omega$ )						
$b$	$a_1$	-15	-23	-22	-27	-25		
$a$	$a_1$	-14	-22	-22	-26	-24		
$a$	$b_2$	-61	-76	-72	-79	-76		
$b$	$b_2$	-61	-75	-71	-78	-75		
		$C_s$ Edge–Edge Frequency Shifts ( $\Delta\omega$ )						
$a''$	$a_1$	-26	-26	-37	-32	-25		
$a'$	$a_1$	-25	-24	-35	-31	-24		
$a''$	$b_2$	-89	-72	-61	-72	-75		
$a'$	$b_2$	-86	-69	-58	-69	-72		
		$C_s$ WW–Edge–Face Frequency Shifts ( $\Delta\omega$ )						
$a'$	$a_1$	-104	-118	-140	-138	-94		
$a'$	$a_1$	-46	-48	-47	-128	-49		
$a'$	$b_2$	-128	-118	-105	-114	-117		
$a''$	$b_2$	-121	-110	-106	-109	-107		

<sup>a</sup>Irreducible representations<sup>76</sup> of the OH stretching mode in the complex (left) and reference mode in H<sub>2</sub>O (right).

dihydrate structure without solvent–solvent interactions was computed to lie  $\approx$ 0.2 kcal mol<sup>-1</sup> lower than any configuration with water–water hydrogen bonding.<sup>57</sup> This study did, however, see spectroscopic evidence emerge for water–water hydrogen bonding in  $\text{SF}_6^-(\text{H}_2\text{O})_3$ .

**3.3. Dissociation Energies.** Table 2 reports the dissociation energies ( $D_e$ ) for the minimum configurations of both the mono- and dihydrate systems (i.e., the relative energy of the isolated, optimized fragments: one  $\text{PF}_6^-$  ion and  $n$  H<sub>2</sub>O molecules). The MP2 and CCSD(T) computations reported here and in ref 23 indicate that the monohydrate minimum ( $C_{2v}$  edge) has a dissociation energy exceeding 10 kcal mol<sup>-1</sup>. For comparison, the  $D_e$  of the water dimer<sup>73,74</sup> is approximately 5 kcal mol<sup>-1</sup> when computed with similar methods and basis sets. Together, these results suggest that the interaction between water and the hexafluorophosphate anion is significantly stronger than the interaction between two neutral water molecules.

The MP2 and CCSD(T) data in Table 2 show that when two edge contacts form in the  $C_s$ ,  $C_{2v}$ , and  $D_{2h}$  edge–edge dihydrate minima, the  $D_e$  increases by a factor of  $\approx$ 1.9 relative to the corresponding value for the monohydrate minimum. As such, the interactions are close to being perfectly additive, but they fall about 5% short of doubling the  $D_e$  of the  $C_{2v}$  edge structure. In contrast, the  $C_s$  WW–edge–face minimum displays cooperative effects that enhance  $D_e$  by roughly 5% to a value slightly larger than 22 kcal mol<sup>-1</sup>.

When the CP procedure is applied to the lowest-energy structures identified for the monohydrate and dihydrate systems ( $C_{2v}$  edge and  $C_s$  WW–edge–face, respectively), the CCSD(T)/haQZ dissociation energies decrease by less than 3% for both. The dissociation energies computed with the CP procedure for these two minima can be found in the Supporting Information, and when they are combined with the CCSD(T) data reported in Table 2, the results indicate that the  $D_e$  of the  $C_{2v}$  edge minimum for  $\text{PF}_6^-(\text{H}_2\text{O})_1$  will be near 10.4 kcal mol<sup>-1</sup> at the CCSD(T) complete basis set limit

339 (where the BSSE must vanish by definition) and that of the  $C_s$   
340 WW-edge-face minimum for  $\text{PF}_6^-(\text{H}_2\text{O})_2$  will be near 22.0  
341 kcal mol<sup>-1</sup>.

342 **3.4. Vibrational Frequencies.** The harmonic symmetric  
343 ( $a_1$ ) and antisymmetric ( $b_2$ ) OH stretching frequencies ( $\omega$ )  
344 computed for an isolated water molecule are listed in the first  
345 two rows of data at the top of **Table 3**. When a water molecule  
346 binds to an edge of the  $\text{PF}_6^-$  octahedron, the formation of the  
347 OH···F hydrogen bonds perturbs the OH stretching vibrations  
348 of the water molecule, inducing a shift in the corresponding  
349 frequency ( $\Delta\omega$ ). In the  $C_{2v}$  edge monohydrate structure, for  
350 example, the energy of the symmetric  $a_1$  stretching mode  
351 decreases by 17 cm<sup>-1</sup> and that of the antisymmetric  $b_2$  mode  
352 decreases by 72 cm<sup>-1</sup>, according to the CCSD(T)/haTZ  
353 results reported in the first column of numbers in **Table 3**. All  
354 of the other methods predict larger shifts with the haTZ basis  
355 set (by approximately 10 cm<sup>-1</sup>). The tabulated MP2 and DFT  
356  $\Delta\omega$  values for the  $C_{2v}$  edge minimum range from -27 to -32  
357 cm<sup>-1</sup> for the  $a_1$  mode and from -83 to -90 for the  $b_2$  mode.  
358 DIHB structures tend to induce less-pronounced OH  
359 stretching frequency shifts in  $\text{H}_2\text{O}$  than their SIHB counter-  
360 parts,<sup>24,25</sup> and the data presented here suggest that the  $C_{2v}$   
361 edge minimum for  $n = 1$  is no exception. In fact, the  
362 magnitudes of the computed harmonic shifts for  $\text{PF}_6^-(\text{H}_2\text{O})_1$   
363 in **Table 3** are appreciably smaller than the readily assignable  
364 shifts from the DIHB series analyzed by Robertson et al. by  
365 more than a factor of two.<sup>24</sup> This result is, however, consistent  
366 with a proton affinity of only 280 kcal mol<sup>-1</sup> for the  
367 hexafluorophosphate anion<sup>75</sup> based on the qualitative relation-  
368 ship between this quantity and the OH frequency shifts (see  
369 **Figure 2** of ref 24, e.g.).

370 For the dihydrate systems, the irreducible representations  
371 associated with the coupled OH stretching vibrations of the  
372 two water molecules are listed in the first column of **Table 3**.<sup>76</sup>  
373 Even when they do not necessarily directly correlate to the  $a_1$   
374 and  $b_2$  irreducible representations of the  $C_{2v}$  point group, each  
375 mode is dominated by a synchronous or asynchronous OH  
376 stretching motion that can be used to assign the  $\text{H}_2\text{O}$  reference  
377 mode for calculating  $\Delta\omega$  (indicated by the  $a_1$  or  $b_2$  entries  
378 tabulated in the second column of **Table 3**).

379 When two water molecules bind to different edges of the  
380 anion octahedron in the dihydrate edge-edge minima ( $D_{2h}$ ,  
381  $C_2$ , and  $C_s$ ), the magnitudes of the vibrational frequency shifts  
382 are quite similar to those observed for the monohydrate. In the  
383 three edge-edge minima, the symmetric OH stretch shifts to  
384 slightly lower energy by  $-19 \pm 7$  cm<sup>-1</sup> according to the  
385 CCSD(T)/haTZ harmonic vibrational frequencies. The  
386 corresponding shifts for the antisymmetric OH stretch also  
387 fall into a fairly narrow range of  $\Delta\omega$  values of  $-75 \pm 14$  cm<sup>-1</sup>.  
388 The similarity of the frequency shifts for the monohydrate  
389 minimum and edge-edge dihydrate minima is consistent with  
390 the lack of cooperative effects observed for the corresponding  
391  $D_e$  values in **Table 2**.

392 With a qualitatively different hydrogen bond topology, the  
393  $C_s$  WW-edge-face structure exhibits much larger OH  
394 stretching frequency shifts than the three Edge-Edge minima.  
395 According to the CCSD(T)/haTZ harmonic vibrational  
396 frequencies, only one OH stretching mode shifts by less than  
397 100 cm<sup>-1</sup>;  $\Delta\omega$  is only -46 cm<sup>-1</sup> for the mode predominated  
398 by the synchronous OH stretching motion in the water  
399 molecule that accepts the OH···O hydrogen bond. In contrast,  
400 the corresponding shift in the donor of the OH···O hydrogen  
401 bond is -104 cm<sup>-1</sup> (both relative to the  $a_1$  stretch of an

402 isolated  $\text{H}_2\text{O}$  molecule). The CCSD(T)/haTZ  $\Delta\omega$  values are 402  
403 -128 and -121 cm<sup>-1</sup> for the asynchronous stretching modes 403  
404 primarily associated with the donor and acceptor of the OH··· 404  
405 O hydrogen bond, respectively.

406 The solvent-solute interactions also induce vibrational 406  
407 frequency shifts in the PF stretching modes of the 407  
408 hexafluorophosphate anion, but they tend to be much smaller 408  
409 (Table S13 in the *Supporting Information*). When a single 409  
410 water molecule interacts with  $\text{PF}_6^-$  to form the  $C_{2v}$  edge 410  
411 monohydrate structure, the CCSD(T)/haTZ harmonic vibra- 411  
412 tional frequencies indicate that one PF stretching frequency 412  
413 shifts by -12 cm<sup>-1</sup> to lower energy, while another shifts by 413  
414 +16 cm<sup>-1</sup> to higher energy, while the four other PF stretching 414  
415 modes shift by no more than  $\pm 7$  cm<sup>-1</sup>. The latter nearly 415  
416 doubles in magnitude to +30 cm<sup>-1</sup> in the  $D_{2h}$  edge-edge local 416  
417 minimum when a second water molecule is added to the 417  
418 opposite side of the  $\text{PF}_6^-$  octahedron. However, the CCSD- 418  
419 (T)/haTZ frequency shifts do not exceed  $\pm 6$  cm<sup>-1</sup> for the 419  
420 lowest-energy structure identified for  $\text{PF}_6^-(\text{H}_2\text{O})_2$  (the  $C_s$  420  
421 WW-edge-face minimum). The vibrational frequency shifts 421  
422 for the PF stretches are tabulated in the *Supporting* 422  
423 *Information* along with all of the computed harmonic 423  
424 vibrational frequencies and corresponding IR intensities. 424

## 4. CONCLUSIONS

425 Low-energy configurations of the  $\text{PF}_6^-(\text{H}_2\text{O})_{n=1,2}$  system have 425  
426 been identified via a set of relaxed angular scans across the 426  
427 edges and faces of the  $\text{PF}_6^-$  octahedron. Two low-lying 427  
428 stationary points have been found for the  $\text{PF}_6^-(\text{H}_2\text{O})_1$  system 428  
429 with the CCSD(T) *ab initio* method, the  $C_{2v}$  Edge minimum 429  
430 and the  $C_s$  transition state. For the  $\text{PF}_6^-(\text{H}_2\text{O})_2$  system, four 430  
431 minima and two transition states have been identified, with the 431  
432 lowest energy minimum being approximately 2 kcal mol<sup>-1</sup> 432  
433 lower than that of any other structure yet identified. 433

434 The CCSD(T) electronic dissociation energy is slightly 434  
435 larger than 10 kcal mol<sup>-1</sup> for the  $C_{2v}$  edge minimum of the 435  
436 monohydrate, and this interaction is almost perfectly additive 436  
437 in the  $D_{2h}$ ,  $C_2$ , and  $C_s$  edge-edge minima of  $\text{PF}_6^-(\text{H}_2\text{O})_2$ . 437  
438 However, appreciable cooperative effects are observed when 438  
439 the two hydrating water molecules are able to interact with 439  
440 each other, and the CCSD(T)  $D_e$  increases to approximately 440  
441 22 kcal mol<sup>-1</sup> for the  $C_s$  WW-edge-face structure. In 441  
442 comparison, the corresponding  $D_e$  is approximately 5 kcal 442  
443 mol<sup>-1</sup> for  $(\text{H}_2\text{O})_2$ ,<sup>73,74</sup> and it approaches 16 kcal mol<sup>-1</sup> for 443  
444  $(\text{H}_2\text{O})_3$ .<sup>77</sup>

445 These solvent-solute interactions also induce significant 445  
446 shifts in the OH stretching vibrational frequencies of the 446  
447 hydrating water molecule(s) relative to the corresponding  $a_1$  447  
448 and  $b_2$  values for an isolated  $\text{H}_2\text{O}$  molecule. The CCSD(T)/ 448  
449 haTZ symmetric and antisymmetric OH stretching frequency 449  
450 shifts by -17 and -72 cm<sup>-1</sup>, respectively, in the  $C_{2v}$  edge 450  
451 monohydrate minimum, and very similar  $\Delta\omega$  values are 451  
452 observed in the  $D_{2h}$ ,  $C_2$ , and  $C_s$  edge-edge minima of 452  
453  $\text{PF}_6^-(\text{H}_2\text{O})_2$ . However, the most significant vibrational 453  
454 perturbations occur when the solvent molecules are able to 454  
455 interact with each other and the ion. In the  $C_s$  WW-edge-face 455  
456 structure, the CCSD(T)/haTZ frequencies shift by as much as 456  
457 -104 cm<sup>-1</sup> for the synchronous and -128 cm<sup>-1</sup> for the 457  
458 asynchronous OH stretching modes. The lowest-energy 458  
459 harmonic OH stretching frequency for the  $C_s$  WW-edge- 459  
460 face minimum of  $\text{PF}_6^-(\text{H}_2\text{O})_2$  is computed to be 3721 and 460  
461 3661 cm<sup>-1</sup> at the CCSD(T)/haTZ and B3LYP/haTZ levels of 461  
462 theory, respectively. The latter harmonic value is only 36 cm<sup>-1</sup> 462

463 larger than the results from recent DFT AIMD simulations that  
464 predicted a shift of more than  $+300\text{ cm}^{-1}$  relative to bulk  
465 water.<sup>21</sup> The present work demonstrates that solvent–solute  
466 interactions alone do not provide a complete picture of  $\text{PF}_6^-$   
467 hydration, and it highlights the importance of the solvent–  
468 solvent interactions that must also be considered to identify  
469 the lowest-energy structures and to capture the associated  
470 spectroscopic perturbations.

## 471 ■ ASSOCIATED CONTENT

### 472 ■ Supporting Information

473 The Supporting Information is available free of charge at  
474 <https://pubs.acs.org/doi/10.1021/acs.jpca.0c06466>.

475 Cartesian coordinates, electronic dissociation energies  
476 computed with the CP procedure, harmonic vibrational  
477 frequencies, and IR intensities ([PDF](#))

## 478 ■ AUTHOR INFORMATION

### 479 Corresponding Author

480 **Gregory S. Tschumper** — *Department of Chemistry and*  
481 *Biochemistry, University of Mississippi, University, Mississippi*  
482 *38677-1848, United States; [orcid.org/0000-0002-3933-2200](https://orcid.org/0000-0002-3933-2200); Phone: +1 662 915 7301; Email: [tschumper@olemiss.edu](mailto:tschumper@olemiss.edu); Fax: +1 662 915 7300*

### 485 Author

486 **Yasmeen A. Abdo** — *Department of Chemistry and*  
487 *Biochemistry, University of Mississippi, University, Mississippi*  
488 *38677-1848, United States*

489 Complete contact information is available at:

490 <https://pubs.acs.org/10.1021/acs.jpca.0c06466>

### 491 Notes

492 The authors declare no competing financial interest.

## 493 ■ ACKNOWLEDGMENTS

494 This work was supported in part by the National Science  
495 Foundation (CHE-1338056 and CHE-1664998). The Mis-  
496 sissippi Center for Supercomputing Research (MCSR) is also  
497 thanked for a generous allocation of time on their computa-  
498 tional resources.

## 499 ■ REFERENCES

- (1) Wang, Y.-L.; Li, B.; Sarman, S.; Mocci, F.; Lu, Z.-Y.; Yuan, J.; Laaksonen, A.; Fayer, M. D. Microstructural and Dynamical Heterogeneities in Ionic Liquids. *Chem. Rev.* **2020**, *120*, 5798–5877.
- (2) Xu, K. Nonaqueous Liquid Electrolytes for Lithium-Based Rechargeable Batteries. *Chem. Rev.* **2004**, *104*, 4303–4418.
- (3) Seddon, K. R.; Stark, A.; Torres, M.-J. Influence of chloride, water, and organic solvents on the physical properties of ionic liquids. *Pure Appl. Chem.* **2000**, *72*, 2275–2287.
- (4) Blanchard, L. A.; Gu, Z.; Brennecke, J. F. High-Pressure Phase Behavior of Ionic Liquid/CO<sub>2</sub> Systems. *J. Phys. Chem. B* **2001**, *105*, 2437–2444.
- (5) Rogers, R. D.; Seddon, K. R. CHEMISTRY: Ionic Liquids—Solvents of the Future? *Science* **2003**, *302*, 792–793.
- (6) Danten, Y.; Cabalo, M. I.; Besnard, M. Interaction of Water Highly Diluted in 1-Alkyl-3-methyl Imidazolium Ionic Liquids with the  $\text{PF}_6^-$  and  $\text{BF}_4^-$  Anions. *J. Phys. Chem. A* **2009**, *113*, 2873–2889.
- (7) Cammarata, L.; Kazarian, S. G.; Salter, P. A.; Welton, T. Molecular States of Water in Room Temperature Ionic Liquids. *Phys. Chem. Chem. Phys.* **2001**, *3*, 5192–5200.
- (8) Ghatee, M. H.; Zolghadr, A. R. Local Depolarization in Hydrophobic and Hydrophilic Ionic Liquids/Water Mixtures: Car-

Parrinello and Classical Molecular Dynamics Simulation. *J. Phys. Chem. C* **2013**, *117*, 2066–2077.

- (9) Huddleston, J. G.; Visser, A. E.; Reichert, W. M.; Willauer, H. D.; Broker, G. A.; Rogers, R. D. Characterization and comparison of hydrophilic and hydrophobic room temperature ionic liquids incorporating the imidazolium cation. *Green Chem.* **2001**, *3*, 156–164.
- (10) Swatloski, R. P.; Visser, A. E.; Reichert, W. M.; Broker, G. A.; Farina, L. M.; Holbrey, J. D.; Rogers, R. D. On the solubilization of water with ethanol in hydrophobic hexafluorophosphate ionic liquids. *Green Chem.* **2002**, *4*, 81–87.
- (11) Hanke, C. G.; Lynden-Bell, R. M. A Simulation Study of Water-Dialkylimidazolium Ionic Liquid Mixtures. *J. Phys. Chem. B* **2003**, *107*, 10873–10878.
- (12) Wang, Y.; Li, H.; Han, S. A Theoretical Investigation of the Interactions between Water Molecules and Ionic Liquids. *J. Phys. Chem. B* **2006**, *110*, 24646–24651.
- (13) Schenck, J.; Panne, U.; Albrecht, M. Interaction of Levitated Ionic Liquid Droplets with Water. *J. Phys. Chem. B* **2012**, *116*, 14171–14177.
- (14) Walrafen, G. E. Raman Spectral Studies of the Effects of Solutes and Pressure on Water Structure. *J. Chem. Phys.* **1971**, *55*, 768–792.
- (15) Paquette, J.; Jolicoeur, C. A near-infrared study of the hydration of various ions and nonelectrolytes. *J. Solution Chem.* **1977**, *6*, 403–428.
- (16) Kristiansson, O.; Lindgren, J.; de Villepin, J. A Quantitative Infrared Spectroscopic Method for the Study of the Hydration of Ions in Aqueous Solutions. *J. Chem. Phys.* **1988**, *92*, 2680–2685.
- (17) Śmiechowski, M.; Gojlo, E.; Stangret, J. Ionic Hydration in LiPF<sub>6</sub>, NaPF<sub>6</sub>, and KPF<sub>6</sub> Aqueous Solutions Derived from Infrared HDO Spectra. *J. Phys. Chem. B* **2004**, *108*, 15938–15943.
- (18) Son, H.; Nam, D.; Park, S. Real-Time Probing of Hydrogen-Bond Exchange Dynamics in Aqueous NaPF<sub>6</sub> Solutions by Two-Dimensional Infrared Spectroscopy. *J. Phys. Chem. B* **2013**, *117*, 13604–13613.
- (19) Nam, D.; Lee, C.; Park, S. A Quantitative Infrared Spectroscopic Method for the Study of the Hydration of Ions in Aqueous Solutions. *Phys. Chem. Chem. Phys.* **2014**, *16*, 21747–21754.
- (20) Śmiechowski, M. Anion-water interactions of weakly hydrated anions: molecular dynamics simulations of aqueous NaBF<sub>4</sub> and NaPF<sub>6</sub>. *Mol. Phys.* **2016**, *114*, 1831–1846.
- (21) Śmiechowski, M. Unusual Influence of Fluorinated Anions on the Stretching Vibrations of Liquid Water. *J. Phys. Chem. B* **2018**, *122*, 3141–3152.
- (22) Stangret, J.; Gampe, T. Ionic Hydration Behavior Derived from Infrared Spectra in HDO. *J. Phys. Chem. B* **2002**, *106*, 5393–5402.
- (23) Rodríguez-Otero, J.; Cabaleiro-Lago, E. M.; Peña-Gallego, Á. Comment on: A Theoretical Investigation of the Interactions between Water Molecules and Ionic Liquids. *J. Phys. Chem. B* **2008**, *112*, 13465–13466.
- (24) Robertson, W. H.; Price, E. A.; Weber, J. M.; Shin, J.-W.; Weddle, G. H.; Johnson, M. A. Infrared Signatures of a Water Molecule Attached to Triatomic Domains of Molecular Anions: Evolution of the H-bonding Configuration with Domain Length. *J. Phys. Chem. A* **2003**, *107*, 6527–6532.
- (25) Woronowicz, E. A.; Robertson, W. H.; Weddle, G. H.; Johnson, M. A.; Myshakin, E. M.; Jordan, K. D. Infrared Spectroscopic Characterization of the Symmetrical Hydration Motif in the SO<sub>3</sub><sup>2-</sup> H<sub>2</sub>O Complex. *J. Phys. Chem. A* **2002**, *106*, 7086–7089.
- (26) Surber, E.; Ananthavel, S. P.; Sanov, A. Nonexistent electron affinity of OCS and the stabilization of carbonyl sulfide anions by gas phase hydration. *J. Chem. Phys.* **2002**, *116*, 1920–1929.
- (27) Myshakin, E. M.; Jordan, K. D.; Sibert, E. L.; Johnson, M. A. Large anharmonic effects in the infrared spectra of the symmetrical CH<sub>3</sub>NO<sub>2</sub><sup>-</sup>(H<sub>2</sub>O) and CH<sub>3</sub>CO<sub>2</sub><sup>-</sup>(H<sub>2</sub>O) complexes. *J. Chem. Phys.* **2003**, *119*, 10138–10145.
- (28) Schneider, H.; Vogelhuber, K. M.; Weber, J. M. Infrared spectroscopy of anionic hydrated fluorobenzenes. *J. Chem. Phys.* **2007**, *127*, 114311.

589 (29) Kelly, J. T.; Ellington, T. L.; Sexton, T. M.; Fortenberry, R. C.;  
590 Tschumper, G. S.; Asmis, K. R. Communication: Gas Phase  
591 Vibrational Spectroscopy of the Azide-Water Complex. *J. Chem.*  
592 *Phys.* **2018**, *149*, 191101.

593 (30) Bentley, J.; Collins, J. Y.; Chipman, D. M. Dissociation of  
594 Ozonide in Water. *J. Phys. Chem. A* **2000**, *104*, 4629–4635.

595 (31) Johnson, M. S.; Kuwata, K. T.; Wong, C.-K.; Okumura, M.  
596 Vibrational spectrum of  $\text{I}^-(\text{H}_2\text{O})$ . *Chem. Phys. Lett.* **1996**, *260*, 551–  
597 557.

598 (32) Ayotte, P.; Weddle, G. H.; Kim, J.; Johnson, M. A. Vibrational  
599 Spectroscopy of the Ionic Hydrogen Bond: Fermi Resonances and  
600 Ion-Molecule Stretching Frequencies in the Binary  $\text{X}^-\cdot\text{H}_2\text{O}$  ( $\text{X} = \text{Cl}$ ,  
601  $\text{Br}$ ,  $\text{I}$ ) Complexes via Argon Predissociation Spectroscopy. *J. Am.*  
602 *Chem. Soc.* **1998**, *120*, 12361–12362.

603 (33) Weber, J. M.; Kelley, J. A.; Nielsen, S. B.; Ayotte, P.; Johnson,  
604 M. A. Isolating the Spectroscopic Signature of a Hydration Shell With  
605 the Use of Clusters: Superoxide Tetrahydrate. *Science* **2000**, *287*,  
606 2461–2463.

607 (34) Weber, J. M.; Kelley, J. A.; Robertson, W. H.; Johnson, M. A.  
608 Hydration of a structured excess charge distribution: Infrared  
609 spectroscopy of the  $\text{O}_2^-\cdot(\text{H}_2\text{O})_n$  ( $1 \leq n \leq 5$ ) clusters. *J. Chem.*  
610 *Phys.* **2001**, *114*, 2698–2706.

611 (35) Robertson, W. H.; Johnson, M. A.; Myshakin, E. M.; Jordan, K.  
612 D. Isolating the Charge-Transfer Component of the Anionic H Bond  
613 Via Spin Suppression of the Intracluster Proton Transfer Reaction in  
614 the  $\text{NO}^-\cdot\text{H}_2\text{O}$  Entrance Channel Complex. *J. Phys. Chem. A* **2002**,  
615 *106*, 10010–10014.

616 (36) Robertson, W. H.; Johnson, M. A. Molecular Aspects of Halide  
617 Ion Hydration: The Cluster Approach. *Annu. Rev. Phys. Chem.* **2003**,  
618 *54*, 173–213.

619 (37) Schneider, H.; Boese, A. D.; Weber, J. M. Unusual hydrogen  
620 bonding behavior in binary complexes of coinage metal anions with  
621 water. *J. Chem. Phys.* **2005**, *123*, 084307.

622 (38) Roscioli, J. R.; Diken, E. G.; Johnson, M. A.; Horvath, S.;  
623 McCoy, A. B. Prying Apart a Water Molecule with Anionic H-  
624 Bonding: A Comparative Spectroscopic Study of the  $\text{X}^-\cdot\text{H}_2\text{O}$  ( $\text{X} =$   
625  $\text{OH}$ ,  $\text{O}$ ,  $\text{F}$ ,  $\text{Cl}$ , and  $\text{Br}$ ) Binary Complexes in the 600–3800  $\text{cm}^{-1}$   
626 Region. *J. Phys. Chem. A* **2006**, *110*, 4943–4952.

627 (39) Kim, J.; Lee, H. M.; Suh, S. B.; Majumdar, D.; Kim, K. S.  
628 Comparative ab initio study of the structures, energetics and spectra  
629 of  $\text{X}^-\cdot(\text{H}_2\text{O})_{n=1-4}$  [ $\text{X} = \text{F}$ ,  $\text{Cl}$ ,  $\text{Br}$ ,  $\text{I}$ ] clusters. *J. Chem. Phys.* **2000**, *113*,  
630 5259–5272.

631 (40) Xantheas, S. S.; Dunning, T. H. Structures and Energetics of  
632  $\text{F}^-(\text{H}_2\text{O})_n$ ,  $n = 1 - 3$  Clusters from *ab Initio* Calculations. *J. Phys.*  
633 *Chem.* **1994**, *98*, 13489–13497.

634 (41) Xantheas, S. S.; Dang, L. X. Critical Study of Fluoride-Water  
635 Interactions. *J. Phys. Chem.* **1996**, *100*, 3989–3995.

636 (42) Ayotte, P.; Nielsen, S. B.; Weddle, G. H.; Johnson, M. A.;  
637 Xantheas, S. S. Spectroscopic Observation of Ion-Induced Water  
638 Dimer Dissociation in the  $\text{X}^-\cdot(\text{H}_2\text{O})_2$  ( $\text{X} = \text{F}$ ,  $\text{Cl}$ ,  $\text{Br}$ ,  $\text{I}$ ) Clusters. *J.*  
639 *Phys. Chem. A* **1999**, *103*, 10665–10669.

640 (43) Chaban, G. M.; Xantheas, S. S.; Gerber, R. B. Anharmonic  
641 Vibrational Spectroscopy of the  $\text{F}^-(\text{H}_2\text{O})_n$  Complexes,  $n = 1, 2$ . *J.*  
642 *Phys. Chem. A* **2003**, *107*, 4952–4956.

643 (44) Baik, J.; Kim, J.; Majumdar, D.; Kim, K. S. Structures,  
644 energetics, and spectra of fluoride-water clusters  $\text{F}^-(\text{H}_2\text{O})_n$ ,  $n = 1 - 6$ :  
645 Ab initio study. *J. Chem. Phys.* **1999**, *110*, 9116–9127.

646 (45) Combariza, J. E.; Kestner, N. R.; Jortner, J. Microscopic  
647 solvation of anions in water clusters. *Chem. Phys. Lett.* **1993**, *203*,  
648 423–428.

649 (46) Combariza, J. E.; Kestner, N. R.; Jortner, J. Energystructure  
650 relationships for microscopic solvation of anions in water clusters. *J.*  
651 *Chem. Phys.* **1994**, *100*, 2851–2864.

652 (47) Xantheas, S. S. Quantitative Description of Hydrogen Bonding  
653 in Chloride-Water Clusters. *J. Phys. Chem.* **1996**, *100*, 9703–9713.

654 (48) Ayotte, P.; Weddle, G. H.; Kim, J.; Johnson, M. A. Mass-  
655 selected “matrix isolation” infrared spectroscopy of the  $\text{I}^-\cdot(\text{H}_2\text{O})_2$   
656 complex: making and breaking the inter-water hydrogen-bond. *Chem.*  
657 *Phys.* **1998**, *239*, 485–491.

658 (49) Bajaj, P.; Zhuang, D.; Paesani, F. Specific Ion Effects on  
659 Hydrogen-Bond Rearrangements in the Halide-Dihydrate Complexes. *J. Phys. Chem. Lett.* **2019**, *10*, 2823–2828.

660 (50) Dorsett, H. E.; Watts, R. O.; Xantheas, S. S. Probing  
661 Temperature Effects on the Hydrogen Bonding Network of the  
662  $\text{Cl}^-(\text{H}_2\text{O})_2$  Cluster. *J. Phys. Chem. A* **1999**, *103*, 3351–3355.

663 (51) Wolke, C. T.; Menges, F. S.; Tötsch, N.; Gorlova, O.; Fournier,  
664 J. A.; Weddle, G. H.; Johnson, M. A.; Heine, N.; Esser, T. K.; Knorke,  
665 H.; et al. Thermodynamics of Water Dimer Dissociation in the  
666 Primary Hydration Shell of the Iodide Ion with Temperature-  
667 Dependent Vibrational Predissociation Spectroscopy. *J. Phys. Chem. A* **2015**, *119*, 1859–1866.

668 (52) Myshakin, E. M.; Jordan, K. D.; Robertson, W. H.; Weddle, G.  
669 H.; Johnson, M. A. Dominant structural motifs of  $\text{NO}^-\cdot(\text{H}_2\text{O})_n$   
670 complexes: Infrared spectroscopic and ab initio studies. *J. Chem. Phys.* **2003**, *118*, 4945–4953.

671 (53) Robertson, W. H.; Diken, E. G.; Price, E. A.; Shin, J.-W.;  
672 Johnson, M. A. Spectroscopic Determination of the  $\text{OH}^-$  Solvation  
673 Shell in the  $\text{OH}^-(\text{H}_2\text{O})_n$  Clusters. *Science* **2003**, *299*, 1367–1372.

674 (54) Chipman, D. M.; Bentley, J. Structures and Energetics of  
675 Hydrated Oxygen Anion Clusters. *J. Phys. Chem. A* **2005**, *109*, 7418–  
676 7428.

677 (55) Wang, X.-B.; Kowalski, K.; Wang, L.-S.; Xantheas, S. S.  
678 Stepwise hydration of the cyanide anion: A temperature-controlled  
679 photoelectron spectroscopy and ab initio computational study of  
680  $\text{CN}^-(\text{H}_2\text{O})_n$ ,  $n = 2 - 5$ . *J. Chem. Phys.* **2010**, *132*, 124306.

681 (56) Gorlova, O.; DePalma, J. W.; Wolke, C. T.; Brathwaite, A.;  
682 Odbadrakh, T. T.; Jordan, K. D.; McCoy, A. B.; Johnson, M. A.  
683 Characterization of the primary hydration shell of the hydroxide ion  
684 with  $\text{H}_2$  tagging vibrational spectroscopy of the  $\text{OH}^-(\text{H}_2\text{O})_{n=2,3}$  and  
685  $\text{OD}^-(\text{H}_2\text{O})_{n=2,3}$  clusters. *J. Chem. Phys.* **2016**, *145*, 134304.

686 (57) Schneider, H.; Weber, J. M. Infrared spectra of  $\text{SF}_6^-\cdot(\text{H}_2\text{O})_n$  ( $n$   
687 = 1 – 3): Incipient reaction and delayed onset of water network  
688 formation. *J. Chem. Phys.* **2007**, *127*, 244310.

689 (58) Lee, C.; Yang, W.; Parr, R. G. Development of the Colle-  
690 Salvetti correlation-energy formula into a functional of the electron  
691 density. *Phys. Rev. B* **1988**, *37*, 785.

692 (59) Grimme, S.; Antony, J.; Ehrlich, S.; Krieg, H. A consistent and  
693 accurate ab initio parameterization of density functional dispersion  
694 correction (DFT-D) for the 94 elements H–Pu. *J. Chem. Phys.* **2010**, *132*, 154104.

695 (60) Zhao, Y.; Truhlar, D. G. The M06 suite of density functionals  
696 for main group thermochemistry, thermochemical kinetics, non-  
697 covalent interactions, excited states, and transition elements: two new  
698 functionals and systematic testing of four M06-class functionals and  
699 12 other functionals. *Theor. Chem. Acc.* **2008**, *120*, 215–241.

700 (61) Chai, J.-D.; Head-Gordon, M. Long-range corrected hybrid  
701 density functionals with damped atom-atom dispersion corrections.  
702 *Phys. Chem. Chem. Phys.* **2008**, *10*, 6615–6620.

703 (62) Dunning, T. H. Gaussian basis sets for use in correlated  
704 molecular calculations. I. The atoms boron through neon and  
705 hydrogen. *J. Chem. Phys.* **1989**, *90*, 1007–1023.

706 (63) Kendall, R. A.; Dunning, T. H.; Harrison, R. J. Electron  
707 affinities of the first-row atoms revisited. Systematic basis sets and  
708 wave functions. *J. Chem. Phys.* **1992**, *96*, 6796–6806.

709 (64) Møller, C.; Plesset, M. S. Note on an Approximation Treatment  
710 for Many-electron Systems. *Phys. Rev.* **1934**, *46*, 618–622.

711 (65) Bartlett, R. J. Coupled-cluster Theory and its Equation-of-  
712 motion Extensions. *WIREs Comput. Mol. Sci.* **2012**, *2*, 126–138.

713 (66) Frisch, M. J.; Trucks, G. W.; Schlegel, H. B.; Scuseria, G. E.;  
714 Robb, M. A.; Cheeseman, J. R.; Scalmani, G.; Barone, V.; Mennucci,  
715 B.; Petersson, G. A.; et al. *Gaussian09* Revision D.01; Gaussian Inc.:  
716 Wallingford CT, 2009.

717 (67) Matthews, D. A.; Cheng, L.; Harding, M. E.; Lipparini, F.;  
718 Stopkowicz, S.; Jagau, T.-C.; Szalay, P. G.; Gauss, J.; Stanton, J. F.  
719 Coupled-cluster techniques for computational chemistry: The  
720 CFOUR program package. *J. Chem. Phys.* **2020**, *152*, 214108.

721 (68) Kestner, N. R. He-He Interaction in the SCF-MO  
722 Approximation. *J. Chem. Phys.* **1968**, *48*, 252–257.

727 (69) Liu, B.; McLean, A. D. Accurate Calculation of the Attractive  
728 Interaction of Two Ground State Helium Atoms. *J. Chem. Phys.* **1973**,  
729 **59**, 4557–4558.

730 (70) Jansen, H. B.; Ros, P. Non-Empirical Molecular Orbital  
731 Calculations on the Protonation of Carbon Monoxide. *Chem. Phys.*  
732 *Lett.* **1969**, **3**, 140–143.

733 (71) Boys, S. F.; Bernardi, F. The Calculation of Small Molecular  
734 Interactions by the Differences of Separate Total Energies. Some  
735 Procedures with Reduced Errors. *Mol. Phys.* **1970**, **19**, 553–566.

736 (72) Tschumper, G. S. Reliable Electronic Structure Computations  
737 for Weak Non-Covalent Interactions in Clusters. *Rev. Comput. Chem.*  
738 **2009**, **26**, 39–90.

739 (73) Tschumper, G. S.; Leininger, M. L.; Hoffman, B. C.; Valeev, E.  
740 F.; Schaefer, H. F.; Quack, M. Anchoring the Water Dimer Potential  
741 Energy Surface with Explicitly Correlated Computations and Focal  
742 Point Analyses. *J. Chem. Phys.* **2002**, **116**, 690–701.

743 (74) Howard, J. C.; Gray, J. L.; Hardwick, A. J.; Nguyen, L. T.;  
744 Tschumper, G. S. Getting down to the fundamentals of hydrogen  
745 bonding: Anharmonic vibrational frequencies of the hetero and  
746 homogeneous dimers of HF and H<sub>2</sub>O from ab initio electronic  
747 structure computations. *J. Chem. Theory Comput.* **2014**, **10**, 5426–  
748 5435.

749 (75) Newton, K. A.; He, M.; Amunugama, R.; McLuckey, S. A.  
750 Selective cation removal from gaseous polypeptide ions: proton vs.  
751 sodium ion abstraction via ion/ion reactions. *Phys. Chem. Chem. Phys.*  
752 **2004**, **6**, 2710–2717.

753 (76) The Gaussian09 conventions for molecular orientation and  
754 irreducible representation assignments were adopted whenever they  
755 differed from the conventions in CFOUR.

756 (77) Anderson, J. A.; Crager, K.; Fedoroff, L.; Tschumper, G. S.  
757 Anchoring the Potential Energy Surface of the Cyclic Water Trimer. *J.*  
758 *Chem. Phys.* **2004**, **121**, 11023–11029.